

tion to 2IQs reduces stride length proportionately and almost abolishes processive movement. We previously showed that the predicted coiled-coil domain of myosin 10 forms a stable single α -helix (SAH) that could contribute to its lever. Sequence comparisons suggested that predicted coiled coil in myosins 6, 7a and *Dictyosporium discoideum* MyoM might also be SAH domains. To test these proposals, we have created a chimera from GFP-myosin 5 2IQ HMM by inserting 112 residues of predicted coiled coil from MyoM after the IQs (2IQ-SAH-HMM). If these residues formed a SAH domain, the lever length would be comparable to the wild type (6IQ) HMM. In single molecule total internal reflection fluorescence assays, 2IQ-SAH-HMM was processive, moving on actin at similar velocity to 6IQ HMM. Step length measurements in this assay showed 2IQ-HMM takes short steps consistent with its truncated lever whereas 2IQ-SAH-HMM takes long steps similar to 6IQ-HMM but with a broader distribution. These data show the MyoM residues can increase step length but allow more choice of target actins. Electron microscopy of metal shadowed 2IQ-SAH-HMM shows a thin SAH domain connecting each 2IQ head to the tail. SAH domain length is consistent with an α -helix of 112 residues, and there is no evidence that it dimerises to form an extension of the myosin 5 coiled-coil tail. We conclude that the predicted coiled coil of MyoM is a SAH domain, and that this domain can contribute to myosin stepping along actin.

Supported by BBSRC and Wellcome Trust.

2277-Pos Electron Microscopy of Myosin 18 Molecules

Kasim Sader¹, Chun Feng Song¹, Yi Yang², James R. Sellers², John Trinick¹

¹Leeds University, Leeds, United Kingdom,

²NHLB Institute NIH, Bethesda, MD, USA.

Board B392

Myosin 18A is a recently identified non-muscle myosin implicated in haematopoiesis. Thus far most of its properties have been inferred from sequence predictions and have not been tested experimentally. The heavy chain C-terminal to the single IQ motif comprises ~700 AA and is mostly predicted to be coiled-coil α -helix. On this basis the molecule was expected to be a dimer with two heads. However, helix propensity plots are less strong than for other myosin tails, such as classes 2 and 5. The α isoform of myosin 18A also contains an N-terminal 300 AA KE-PDZ sequence. We have studied the shape and flexibility of myosin 18A by negative stain electron microscopy. Both α and β isoforms of HMM (truncated at residue 1363) were dimeric. Image averages of expressed α isoform heads showed extra density that may be the KE-PDZ domain near where the N-terminus is expected. The α isoform heads also bundled actin in the presence or absence of ATP, but this was not observed for the β isoform. The tail of the full length molecule was 96 \pm 8 nm long, which is approximately what is predicted for the coiled-coil. The full length molecule also formed bipolar filaments at roughly physiological ionic strength. The results are consistent with the suggestion that the tail region of myosin 18 has similarities to class 2 myosins.

Myosin & Myosin-family Proteins - II

2278-Pos Fluorescent Probes on the N-terminal Domain of the Regulatory Light Chain of Smooth Muscle Myosin: Kinetics of Nucleotide Binding

Guizhi Song, Patricia A. Ellison, Christine R. Cremo

University of Nevada School of Medicine, Reno, NV, USA.

Board B394

Previous studies¹ showed that nucleotide binding to unphosphorylated smooth muscle heavy meromyosin (UP-HMM) with acrylodan-labeled A23C on the regulatory light chain (RLC), increased the polarity and decreased the solvent exposure of the fluorophore, but not in S1 or in phosphorylated HMM (TP-HMM). This suggests that the acrylodan signal is specific to constructs that are regulated by phosphorylation. Here we further investigate the relationship between nucleotide binding kinetics as measured by tryptophan fluorescence *versus* that measured by acrylodan. We show that the second order rate constant for ATP binding reported by tryptophan (K_1k_{+2}) is the same in S1, UP-HMM and P-HMM. It is similar to the fast phase of a biphasic response of acrylodan to [ATP]. Interestingly, the total amplitude change is greater for UP-HMM (–8%) with an acrylodan on both heads than for UP-HMM with acrylodan on only one head (–2%). This suggests a mechanism of ATP-induced self-quenching of the fluorophores, requiring proximity. We propose that A23 in UP-HMM and P-HMM are in similar environments, but only in UP-HMM can ATP cause the two fluorophores to self-quench. In relation to ADP binding, we report a biphasic response of tryptophan fluorescence, only in HMM not in S1. The second order rate constant for ADP binding as measured by tryptophan was similar for S1, UP-HMM and P-HMM. Acrylodan fluorescence changes in response to ADP are still under investigation. Fluorescence anisotropy experiments are underway to determine whether nucleotide can induce changes in rotational mobility of acrylodan at A23C and other positions within the N-terminal domain.

References

1. Mazhari, S. M., Selser, C. T. & Cremo, C. R. *J Biol Chem* **279**, 39905–14 (2004).

2279-Pos The Mechanism of Blebbistatin Inhibition on Actin-Myosin Mechanics

Anneka M. Hooft, Ryan D. Smith, Steven F. Shannon, Kevin C. Facemyer, Christine R. Cremo, Josh E. Baker

University of Nevada, Reno, NV, USA.

Board B395

Blebbistatin is a small molecule inhibitor of both muscle force and unloaded shortening. Its primary kinetic effect is to trap myosin in a products complex that has a low affinity for actin. However, the link between blebbistatin's mechanical and kinetic effects remains

unclear. Using an *in vitro* motility assay, we demonstrate that blebbistatin inhibits actin sliding velocities ($V = d/\tau_{on}$) by reducing myosin's apparent step size, d , without affecting the time myosin spends strongly bound to actin, τ_{on} . Using a sedimentation binding assay, we demonstrate that upon addition of blebbistatin, the actin-myosin affinity, $-\Delta G_b$, decreases proportionally with d . These results support a thermodynamic model of muscle contraction in which actin sliding is driven by actin-myosin binding energetics and is viscous-limited rather than strictly detachment-limited. In other words, V varies proportionally with F_{uni}/τ_{on} , where F_{uni} is the unitary driving force generated by individual myosin molecules and varies linearly with $-\Delta G_b$. We use analytical and molecular models to better understand the implied relationship between d , F_{uni} and ΔG_b . Beyond elucidating the mechanism of blebbistatin inhibition of actin-myosin mechanics, these studies provide novel insights into basic molecular mechanisms of muscle contraction.

2280-Pos The Effects of Myosin Regulatory Light Chain Phosphorylation on Striated Muscle Myosin Motility and Force Production

Michael Greenberg¹, Kiran Pant¹, James Watt¹, Tanya Mealy¹, Michelle Jones², Danuta Szczesna-Cordary², Jeffrey Moore¹

¹ Boston University, Boston, MA, USA,

² University of Miami, Miami, FL, USA.

Board B396

The regulatory light chain (RLC) of myosin, which binds to the alpha helical neck region of myosin, contains a phosphorylatable serine that is the substrate for myosin light chain kinase. Phosphorylation of the RLC in smooth and non-muscle myosin regulates myosin's enzymatic activity whereas in striated muscle, the myosin is active unless sterically blocked from associating with actin by thin filament regulatory proteins. Phosphorylation of the RLC in striated muscle has been proposed to cause the myosin heads to move away from the thick filament backbone (Sweeney et al. *Am. J. Physiol.* 1993) and has been correlated with increased force at submaximal calcium activation (Persechini et al., *JBC* 1989) and an increase in isometric tension (Szczesna, et.al., *J. Appl. Physiol.*, 2002; Davis et al., *Cell* 2001) in fibers. Here, we examined the effects of striated muscle myosin RLC phosphorylation on thin filament regulation and duty cycle in motility assays and the effect on isometric force using an optical-trap-based force assay (See also Pant et al. *BPS Abstract* 2008). We show that while there is no change in myosin regulation or duty cycle upon phosphorylation, there is a significant increase in isometric force for myosins with phosphorylated RLCs. These results are consistent with an increase in unitary force, agreeing with the increase in force seen in the fiber data.

Supported by NIH-HL077280, AHA-0435434T (J.R.M.) and NIH-HL071778 (D.S.-C.).

2281-Pos Multi-Scale Modeling and Refinement Against Electron Microscopy Data: The Molecular Activation of Tarantula Thick Filaments

Willy Wriggers^{1,2}, Lorenzo Alamo³, Raúl Padrón³

¹ D. E. Shaw Research, New York, NY, USA,

² Weill Cornell Medical College, New York, NY, USA,

³ IVIC, Caracas, Venezuela.

Board B397

Coarse-grained models facilitate the structural refinement of molecular fragments in large macromolecular complexes. The components of such complexes undergo a wide range of motions, and shapes observed at low resolution often deviate from the known atomic structures. We have developed a coarse-grained model for the refinement of the atomic structure of the myosin filament against cryo-EM data of tarantula muscle at 20 Å resolution. EM of smooth and striated muscle myosin provided insight into the relaxed (switched-off) myosin structure, achieved by asymmetric intramolecular interactions between both heads. Cryo-EM reconstruction and flexible fitting reveals two new contacts: one between the free-head and its S2, and another between the free-head and the neighbor blocked-head. The atomic structure is allowed to move according to displacements tracked by 31 control points judged by us to be sufficient for capturing the shape details. Our conservative choice of 31 points (corresponding to a spatial resolution of 27 Å) is slightly below the nominal resolution to avoid an overfitting of the data. We applied molecular dynamics simulations to flexibly fit an interacting-heads atomic model that included the tarantula RLC homology model, its 52aa N-terminal fragment predicted model and the human cardiac S2 crystal structure. The fitting revealed an intramolecular interaction between the cardiomyopathy loop (Arg-411) of the free-head and its S2 and one intermolecular interaction between the 297–326 loop of the free-head with the N-terminal fragment of the blocked-head regulatory light chain. These intermolecular interactions help to establish the thick filament switched-off (relaxed) state. Phosphorylation of Ser-45 of the RLC N-terminal fragment could weaken this intermolecular interaction, as suggested by secondary structure predictions, helping to release both heads during activation of the thick filament.

2282-Pos Actin-Binding Cleft Closure in Myosin II Probed by Site-Directed Spin Labeling

Jennifer C. Klein, Margaret A. Titus, David D. Thomas

Univeristy of Minnesota, Minneapolis, MN, USA.

Board B398

Here we present a new, structurally dynamic, model for nucleotide- and actin-induced closure of the actin-binding cleft of myosin, based on site-directed spin labeling experiments on *Dictyostelium* myosin II. Single-cysteine mutants were engineered and spin-labeled to probe mobility and accessibility of key sites within the

cleft. For most of these sites, addition of ADP and vanadate, to trap the post-hydrolysis state, decreased probe mobility and accessibility slightly, while actin binding caused more dramatic decreases. To measure distances across the cleft, we engineered pairs of cysteine labeling sites to straddle the cleft, with one label on the upper 50 kDa domain and a second on the lower 50 kDa domain. Distances between these spin-labeled sites were determined from the resulting spin-spin interaction, as measured by CW-EPR for distances 7–20 Å or pulsed EPR (DEER) for distances 17–60 Å. We find that (1) three distinct cleft conformations are resolved at inner cleft sites corresponding to ‘open,’ ‘partially closed,’ and ‘closed,’ (2) all biochemical states tested reflect a mixture of conformations, even the rigor actomyosin complex and (3) far outer cleft sites are sensitive to the counterclockwise rotation of the upper 50 kDa relative to the lower 50 kDa that ‘closes’ the cleft. In the apo state, several conformations were resolved, only one of which agreed with the crystal structure. In the post-hydrolysis state, this conformational heterogeneity diminished and distance changes were consistent with partial cleft closure. Actin binding induced more dramatic distance changes, consistent with further cleft closure, but all three conformational states are populated. The resulting picture is much more dynamic than previously envisioned, with both “open” and “closed” cleft conformations interconverting, even in the rigor actomyosin complex.

This work was supported by NIH (AR32961) and the Minnesota Supercomputing Institute.

2283-Pos Using a Bifunctional Spin Label to Measure the Orientation and Dynamics of Myosin in Muscle Fibers

Andrew R. Thompson¹, Ryan N. Mello¹, Nariman Naber², Roger Cooke², David D. Thomas¹

¹University of MN, Minneapolis, MN, USA,

²UCSF, San Francisco, CA, USA.

Board B399

Previous efforts to measure the dynamics and orientation of the muscle motor protein myosin have used monofunctionally attached spin labels (Cooke, et al., 1982; Roopnarine and Thomas 1995, and Baker et al. 1998). However, due to the probe’s monofunctional coupling and its inherent mobility, the spectra report a combination of both protein and probe states. In order to make more precise measurements of myosin’s orientation and dynamics, we have used a bifunctionally attached methanethiosulfonate spin label (BSL) to examine myosin filaments. We have used this spin label to crosslink SH1 and SH2 in the myosin catalytic domain (CD) and found that the spectra report extremely strong immobilization (correlation time greater than 0.1 ms, detected by saturation transfer EPR) but high orientational disorder (detected by conventional EPR of oriented muscle fibers). This may represent a long-sought weakly bound intermediate state in the actomyosin ATPase cycle. To determine whether this disorder in the CD extends to the light-chain domain (LCD), we have measured myosin head orientation using FDNASL attached to cysteine 108 on the regulatory light chain (RLC), then crosslinked SH1 and SH2 with pPDM. The orientational order of the light chain domain (LCD), detected by FDNASL, is only partially

decreased by pPDM crosslinking. We conclude that the weak-binding state trapped by SH1-SH2 crosslinking is highly disordered at the interface between actin and the myosin CD, but only partially disordered at the distal LCD.

This work was supported by NIH (AR32961, AG26160, AR007612) and the Minnesota Super Computing Institute.

2284-Pos Oscillatory Instability Of An Collection Of Non Processive Molecular Motors

Pierre-Yves PLACAIS, Pascal Martin

Institut Curie, PARIS, France.

Board B400

Hair cells from the inner hear of the vertebrate can power spontaneous oscillations of their mechanosensory hair bundles, thereby enhancing their sensitivity to small stimuli at frequencies close to that of the spontaneous oscillation. A mechanism proposed to explain the oscillatory instability involves, in each stereocilium of the bundle, a group of non processive myosins (myosin 1c) that exert force on a mechanosensitive ion channel. Muscle sarcomeres, another sytem involving a collection of non processive myosins II, have also been shown to exhibit oscillatory contractile behaviour under non physiological conditions.

We designed in vitro experiments to mimic the geometry of those two systems. We first showed that it was possible to get oscillations with a simple system including only HMM, actin, and an elastic restoring force opposing the active force generated by the motors. We also investigated the force-velocity relation of such a motor assembly and showed that non linear friction could lead to the observed oscillatory instability.

2285-Pos Intrinsic Probes of Loop 1 Structural Dynamics in Smooth Muscle Myosin

Christopher L. Berger, Justin Decarreau, Scott Barbick, Andrew Kasparsin, Lynn Chrin

University of Vermont, Burlington, VT, USA.

Board B401

Loop 1 is a flexible loop linking the N-terminal 25 kD- and 50 kD-subdomains of the myosin motor domain. Mutagenesis studies have implicated a role for loop 1 in modulating the rate of product release from the myosin active site, but the mechanisms by which loop 1 does this are largely unknown. Crystallographic studies of multiple myosin isoforms have provided little information regarding the conformation of loop 1 in any intermediate state of the enzymatic ATPase cycle due to a lack of electron density resulting from its highly flexible structure. To investigate the structural dynamics of this important component of the smooth muscle myosin motor domain we have genetically engineered a construct containing a single tryptophan residue in loop (F215W). Steady-state measure-

ments of the intrinsic fluorescence from F215W demonstrate that loop 1 adopts multiple conformations as it proceeds through its ATPase cycle. Fluorescence resonance energy transfer (FRET) experiments are on-going to further elucidate the conformational state of loop 1 in the presence of different nucleotides and nucleotide analogs. The structural dynamics of loop 1 may help explain myosin's ability to bind both actin and ADP relatively tightly despite the tight coupling between conformations of the actin-binding cleft and active-site, which results in a reciprocal relationship between myosin's affinity for actin and ATP. Transient kinetic studies following the intrinsic fluorescence changes from F215W will help further define loop 1's modulatory role of ADP release in the absence and presence of actin.

2286-Pos Probing The Rabbit Skeletal Nucleotide Pocket In Rigor Fibers Under Isometric Load Using EPR Spin Labeled Nucleotides

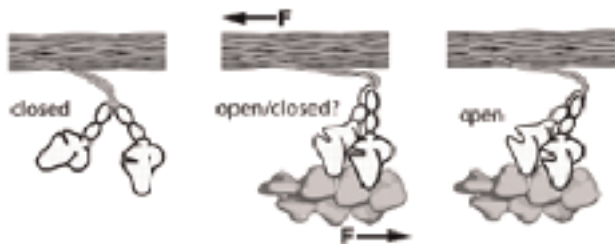
Thomas J. Purcell¹, Nariman Naber¹, Edward Pate², Roger Cooke¹

¹ University of California, San Francisco, San Francisco, CA, USA,

² Washington State University, Pullman, WA, USA.

Board B402

Myosin undergoes conformational changes upon binding to actin. Part of the progression to a post stroke rigor conformation involves opening the conserved switch 1 and switch 2 regions that enclose the nucleotide pocket. Previous studies using spin labeled nucleotides have shown that actomyosin SLADP is primarily open, although there is an equilibrium between open and closed states. The distribution of open and closed states could be related to potential strain sensing mechanisms leading to efficient use of nucleotide under isometric conditions. We have begun studies looking at the nucleotide state under isometric conditions. Rabbit skeletal fiber bundles were labeled using 2'SLATP. We suspended labeled bundles inside the EPR cavity under 30–200 kN m⁻² load. EPR spectra were analyzed by deconvolution into three component spectra corresponding to spin label bound in an open or closed nucleotide pocket and unbound nucleotide. The ratio of open to closed nucleotide pocket is used to calculate the deltaG for nucleotide pocket. Initial studies with both fast and slow skeletal muscle fibers do not show a change in the nucleotide pocket under load.



2287-Pos Intrinsic Probes of Switch I Conformational Changes in Smooth Muscle Myosin

Lynn Chrin, Chauca English, Scott Barbick, Andrew Kasprisin, Justin Decarreau, Christopher Berger

University of Vermont, Burlington, VT, USA.

Board B403

Switch I, a flexible loop in the myosin active site, is believed to coordinate the enzymatic ATPase activity of the motor protein with its affinity for actin. To further elucidate the role of Switch I in coordinating the enzymatic functions of smooth muscle myosin, we have constructed a series of mutants containing a single tryptophan residue around Switch I (F234W, F248W, F251W). Fluorescence intensity and λ_{max} values of F234W-MDE are almost completely insensitive to the addition of ADP or ATP. Fluorescence intensity decreases by 16% and 21% in F251W-MDE in the presence of ADP and ATP, respectively, without a significant change in λ_{max} . F248W-MDE shows the most interesting changes in response to nucleotide, with a 15% increase in intensity and 11 nm blue-shift in the presence of ATP, and a 25% decrease in intensity with a 5 nm blue-shift in the presence of ADP. All three mutants show significant changes in the distance from W234, W248 or W251 and a fluorescent *mant* group on the ribose ring of adenine nucleotide analogs upon phosphate release. Thus we have identified spectroscopic signatures that can be used to follow dynamic changes in switch I during the myosin II ATPase cycle. Initial experiments following changes at F251W indicate two structural transitions in the Switch I following ATP binding, a fast (496 s⁻¹) nucleotide-dependent phase and a slow (6.2 s⁻¹) nucleotide-independent component. We interpret the latter to be a slow isomerization between two conformations prior to nucleotide binding, and former to be a fast isomerization upon the actual binding of ATP.

2288-Pos Muscle and Non-muscle Myosin II Force-generating Domain Probed at SH1 by Spin-label EPR

Roman V. Agafonov, Margaret A. Titus, David D. Thomas, Yuri E Nesmelov

University of Minnesota, Minneapolis, MN, USA.

Board B404

Site-directed spin labeling and EPR spectroscopy were used to characterize the local structure of muscle (rabbit skeletal) and non-muscle (*Dictyostelium discoideum*) myosin II in the region of force generation. It has previously been shown that an iodoacetamide spin label [4-(2-Iodoacetamido)-TEMPO] can be attached specifically to Cys 707 (designated SH1) in muscle myosin, yielding spectra that resolve the key structural intermediates in the ATPase reaction cycle. SH1 is in close proximity to the key structural elements involved in force generation: SH1 helix, relay helix, N-terminal domain, and converter domain. In order to obtain EPR data from an equivalent site in non-muscle myosin, the T688C mutation was

introduced into a Cys-lite construct of the *Dicty* myosin II motor domain. EPR spectra of both SH1-spin-labeled myosins were recorded in the apo state (no nucleotide), as well as in the presence of ADP and nucleotide analogs (ADP.Vi, ADP.BeF_x, ADP.AIF₄). Qualitatively, muscle and *Dicty* myosins showed similar responses: nucleotides increased spin label mobility and resolved three spectral components, corresponding to three distinct structural states. However, there were quantitative differences in the spectra of the two myosins in the presence of nucleotide analogs. Digital spectral analysis revealed that the three spectral components were virtually identical in the two myosins, indicating that the three structural states are also similar in the vicinity of the probe. Thus the difference between the two myosins is in the mole fractions of these structural states. These results suggest that the principal differences between muscle and *Dicty* myosins are kinetic, not structural, and they establish the groundwork for further spectroscopic analysis of *Dicty* myosin, probing other sites and functional mutations.

[Supported by NIH Grant AR32961 to DDT, NIH Grant AR53562 to YEN and by University of Minnesota Supercomputing Institute].

2289-Pos Modification of Myosin Function by Nitric Oxide and Nitrosothiols

Alicia M. Evangelista¹, Vijay S. Rao¹, Allan Doctor², Benjamin M. Gaston¹, William H. Guilford¹

¹ University of Virginia, Charlottesville, VA, USA,

² Washington University, St. Louis, MO, USA.

Board B405

Nitric oxide (NO) has long been recognized as a signaling molecule influencing muscle contraction. The mechanism of regulation is both via activation of guanylyl cyclase, and S-nitrosation of proteins. However, the breadth and importance of the nitrosated targets remain to be fully understood. We tested the hypothesis that skeletal and cardiac muscle myosins are directly regulated by nitric oxide and small, endogenous nitrosothiols. The velocities of actin filaments over rat skeletal and cardiac muscle myosins were measured in a reducing agent-free motility assay after exposure to diethylamine (DEA) NONOate, a NO donor, or s-nitrosocysteine (SNO-cys). Both DEA NONOate and the L-isomer of nitrosocysteine (SNO-L-cys) reduced velocities over cardiac and skeletal myosins and HMM in a dose-dependent fashion. In contrast, the D-isomer of SNO-cys had no effect on actin filament velocity; thus, the effect of nitrosothiols on myosin was stereospecific. The effect of SNO-L-cys on actin filament velocity was reversible by exposure to ultraviolet light, strongly suggestive of nitrosation as the underlying modification. Donor-treated myosin was mixed with untreated myosin in the motility assay to determine the relative change in force generating capacity. These mixtures assays suggested an approximate 2-fold increase in force generation subsequent to donor exposure. This conclusion is supported by preliminary data from a laser trap assay for measuring isometric force that also suggest an increase in force subsequent to NO exposure. These data support a strong yet nuanced effect of NO on skeletal and cardiac myosins that extends beyond mere inhibition and suggest that NO may act as a "gear shift" for

myosin, regulating it toward lower velocity but higher force. We suggest that myosin is directly regulated by S-NO modifications of the reactive sulfhydryls, cys697 and cys707, both of which are surrounded by a putative nitrosylation motif.

2290-Pos *Drosophila* Skeletal Muscle Myosin Converter And Relay Loop Interaction Is Important For Enzymatic Activity, Thermal Stability, Actin Sliding Velocity, Myofibril Stability And Flight Ability

Girish C. Melkani, William A. Kronert, Anju Melkani, Aileen F. Knowles, Sanford I. Bernstein

San Diego State University, San Diego, CA, USA.

Board B406

We generated a transgenic *Drosophila* line to explore the interaction between the relay loop and converter domains of skeletal muscle myosin. Site directed mutagenesis was carried out on pwMhc2, a wild-type *P* element construct, to replace arginine 758 with glutamic acid. This residue is located in the indirect flight muscle (IFM) specific converter domain (encoded by exon 11e). The charge change in the mutated line, IFIE11e, is predicted to disrupt interaction with isoleucine 508 located in the relay loop domain (encoded by exon 9a). Both basal and actin stimulated Mg²⁺-ATPase activity of full-length myosin or S-1 (myosin head) of the mutant were reduced ~ 60 % compared to pwMhc2. Actin sliding velocity of the mutant was reduced ~ 40% compared to pwMhc2. Furthermore, mutant myosin or S-1 was highly susceptible to denaturation at elevated temperature (37°C), as indicated by rapid loss of ATPase activity and increased aggregation kinetics in the mutant compared to pwMhc2. Transmission electron microscopy was used to examine the ultrastructure of the IFM during different stages of development. IFIE11e showed normal myofibril assembly, myofibril shape, and normal hexagonal arrangement of thick and thin filaments in pupae and two-day-old flies. One-week-old adult IFIE11e showed subtle cracking and frayed myofibrils with mild disruption of the hexagonal arrangement of the thick and thin filaments compared to pwMhc2. Flight ability was severely compromised in two-day old IFIE11e adults and absent at one week. Our results demonstrate the importance of residue arginine 758 in myosin and muscle function. Furthermore, our study suggests that proper interaction of the converter domain with the relay loop domain is critical for the mechanochemical functioning of myosin.

2291-Pos Mapping the Actin-Myosin Interface by Site-Directed FRET

Piyali Guhathakurta, Vicci L. Korman, Ewa Prochniewicz, David D. Thomas

Department of Biochemistry, Molecular Biology, and Biophysics University of Minnesota, Minneapolis, USA

Board B407

The molecular mechanism of muscle contraction involves transitions of the actin-myosin complex between weak and strong binding states. To characterize the interface between these two proteins, we have applied site-directed fluorescence resonance energy transfer (FRET) to determine distances between specific sites in actin and myosin. We have engineered labeling sites in yeast actin and Dictyostelium myosin II motor domain (S1dC) by introducing cysteine residues at the proposed sites of weak and strong binding. Cosedimentation binding assays indicate that the labeled mutant proteins bind stoichiometrically. Distances were measured under rigor conditions (no ATP) between yeast actin labeled with a donor probe IAEDANS at residues Cys5 (weak binding site) or Cys345 (strong binding site) to myosin residues Cys401 (strong binding site) or Cys619 (weak binding site) labeled with an acceptor probe, 5 IAF. The FRET distances from Cys5 of actin to Cys401 and Cys619 of myosin are 39 ± 1 Å and 38 ± 1 Å respectively. These and other distances will be used to map the actin-myosin interface in order to improve the current structural models of the actin-myosin complex in both weak- and strong-binding states.

This work was supported by grants from NIH (AR32961) and the Minnesota Supercomputing Institute.

2292-Pos Removal of the Cardiac Myosin Regulatory Light Chain Increases Isometric Force Production

Kiran Pant¹, James D. Watt¹, Tanya R. Mealy¹, Michael J. Greenberg¹, Michelle Jones², Danuta Szczesna-Cordary², Jeffrey R. Moore¹

¹ Boston University, Boston, MA, USA,

² University of Miami School of Medicine, Miami, FL, USA.

Board B408

The myosin neck, which is supported by the interactions between light chains and the underlying α -helical heavy chain, is thought to act as a lever arm to amplify movements originating in the globular motor domain. It has been shown that the removal of the regulatory light chains (RLCs) from muscle fibers or from isolated myosin significantly reduces maximum unloaded shortening velocity, with little effect on isometric force for skeletal muscle myosin. Here, we studied the role of RLCs in cardiac myosin's capacity to produce force and motility using frictional loading and optical-trap based isometric force *in vitro* motility assays. We measured the isometric force and actin filament velocity for native porcine cardiac myosin (PC), RLC depleted myosin PC_{depl} and myosin reconstituted with bacterially expressed human RLC (PC_{recon}). The removal of RLC reduced the maximum unloaded shortening velocity of myosin by ~50% and enhanced the isometric force by 50%, while reconstitution with human RLC restored the velocity and force levels to near untreated values. The reduction in unloaded velocity after RLC extraction is consistent with the myosin neck acting as a lever. While duty cycle measurements and surface ATPase assays indicate that the enhancement in isometric force can be directly related to enhancement in unitary force. Our force data support a model in

which the neck region behaves as a cantilevered beam with force being inversely proportional to the square of neck length.

Supported by NIH-HL077280 and HL086655 (J.R.M.) and NIH-HL071778 (D.S.-C.).

2293-Pos The Effects of Regulatory Light Chain Cardiomyopathy Mutations on Myosin Mechanics and Kinetics

Michael J. Greenberg¹, James D. Watt¹, Michelle Jones², Danuta Szczesna-Cordary², Jeffrey R. Moore¹

¹ Boston University School of Medicine, Boston, MA, USA,

² University of Miami School of Medicine, Miami, FL, USA

Board B409

The myosin head domain consists of a globular domain and an elongated α -helical neck region, which is thought to undergo large conformational changes during the production of force and motion. The myosin regulatory light chain (RLC) functions to support the neck region, therefore it is not surprising that several single amino acid substitutions in the RLC have been implicated in familial hypertrophic cardiomyopathy (FHC), the leading cause of sudden cardiac death in young adults. To examine the effect of these mutations on myosin mechanics and kinetics, we purified myosin from transgenic mice expressing FHC mutations near the calcium binding site of the RLC (R58Q and N47K) and near the N- and C-termini of the RLC (F18L and D166V respectively). We used *in vitro* motility assays to probe the velocity, duty cycle, and force generating capabilities of the mutant myosins. Frictional loading assays indicate a reduction in myosin isometric force in all of the mutations. While the relationship between myosin surface density and velocity indicate no change in duty cycle for N47K and an increase in duty cycle for R58Q, which agrees with data obtained with skinned fibers (*JMB* (361) 2006 p. 286). These results are consistent with the RLC mutations affecting myosin unitary force.

Supported by NIH-HL077280 and P01HL086655 (J.R.M.) and NIH-HL071778 (D.S.-C.).

2294-Pos The Cross-bridge Kinetics of Slow, Medium, Very Fast and Superfast *Drosophila* Myosin Isoforms Under Unloaded Conditions

Catherine Eldred, Dimitre Simeonov, Chaoxing Yang, Douglas M. Swank

Rensselaer Polytechnic Institute, Troy, NY, USA.

Board B410

Our recent experiments suggest the critical kinetic adaptations of the *Drosophila* superfast IFM myosin isoform (IFI) for high speed oscillatory work generation are an extremely fast detachment rate of

myosin from actin, a weak affinity of MgATP for myosin, and a rate limiting step in the cross bridge cycle at the point of phosphate release¹. In contrast, when the IFM expresses the much slower EMB myosin isoform, our data suggest an isomerization associated with MgADP release is rate limiting. We hypothesize that in superfast muscles MgADP release is sped up to where Pi release becomes rate limiting. To test if these myosin kinetic adaptations also occur under maximum velocity conditions, we are using the *in vitro* motility assay and have developed the *Drosophila* jump muscle (tergal depressor of trochanter) preparation to measure the actin velocity and shortening velocity of 4 different speed *Drosophila* myosin isoforms. Preliminary analysis of actin filaments propelled by IFI myosin suggests a V_{\max} of about 6 $\mu\text{m}/\text{sec}$ at 25°C, 50 mM ionic strength, and a K_m about 0.1 mM ATP. Addition of phosphate (Pi) up to 8 mM does not appear to affect IFI actin velocity. Pi slightly decreases shortening velocity of wild type TDT muscle from $6.1 \pm 0.3 \text{ ML/s}$ at 0 mM Pi to $4.5 \pm 0.3 \text{ ML/s}$ at 20 mM Pi, 15°C. The TDT K_m for velocity and MgATP is about 1.3 mM. In contrast, TDT expressing the slow myosin, EMB, has a K_m around 0.8 mM, a V_{\max} of $3.6 \pm 0.4 \text{ ML/s}$, and increasing [Pi] has no effect on shortening velocity. Tension decreases with increasing [Pi] for both wild type and EMB TDT fibers.

References

1. D. Swank *et al. Proc. Natl. Acad. Sci.* 46, 17543 (2006).

2295-Pos A Myosin Motor that Selects Bundled Actin

Stanislav Nagy, Benjamin L. Ricca, Ronald S. Rock

University of Chicago, Chicago, IL, USA.

Board B411

Eukaryotic cells organize their contents through trafficking along cytoskeletal filaments. The leading edge of a typical metazoan cytoskeleton consists of a dense and complex arrangement of cortical actin. A dendritic mesh is found across the broad lamello-podium, with long parallel bundles at microspikes and filopodia. It is currently unclear if and how myosin motors identify the few actin filaments that lead to the correct destination, when presented with many apparently similar alternatives within the cortex. In this work we show that myosin X, an actin-based motor that concentrates at the distal tips of filopodia, favours the fascin-actin bundle structure at the filopodial core for motility. Expressed dimeric myosin X moves poorly on individual actin filaments, often forming plectonemes in a filament gliding assay as if it travels on a helical path. However, single myosin X motors move robustly and processively along fascin-actin bundles. Furthermore, motility is not only supported, but also enhanced on actin that is tightly ordered without any bundling protein. Our results demonstrate that myosin X recognizes the local structural arrangement of parallel unidirectional filaments in long bundles, providing a mechanism for its specific function and localization. More generally, this work introduces a novel adaptation strategy of molecular motors that provides insight into how certain motors are tuned for their unique roles in cellular function.

2296-Pos Murine Myogenic Cells Express A Slow Or A Mixed (fast/slow) Myosin Heavy Chain (mhc) Profile Following Differentiation *In Vitro*

Lucy M. Colman, Edward White, Michelle Peckham

University of Leeds, Leeds, United Kingdom.

Board B412

Skeletal muscle fibres differ on the basis of muscle specific protein isoform expression, contractile properties and in their metabolism. Satellite cells, found under the basement membrane of muscle fibres are responsible for growth and regeneration following injury or disease. The aim of this research was to determine if myotubes derived from single satellite cells exhibited a similar variation in their phenotype compared to mature muscle fibres. We used myogenic clones derived from satellite cells of several muscles from the transgenic immortal mouse. 5–10 day old myotubes differentiated from six different clones were analysed for myosin heavy chain isoform composition and contractile properties. The clones were derived from either neonatal (mixed limb muscle), or 6–12 week *Extensor Digitorum Longus* (EDL), *Longissimus Dorsi* (LD) or *Soleus* muscle. Overall, clones derived from predominantly slow-oxidative muscle (*Soleus*) differentiated into myotubes that only expressed slow myosin heavy chain isoforms (MHC1), whereas clones derived from predominantly fast-glycolytic (EDL or LD) or neonatal muscles expressed both fast and slow myosin isoforms (MHC1, MHC2a or MHC2b). We compared the time to peak shortening (*ttp*), and time to half relaxation ($t_{0.5}$) during a twitch contraction, using video edge detection of stimulated myotubes. All the clones had generally similar values for both *ttp* and $t_{0.5}$. The average values for *ttp* and $t_{0.5}$ were $189 \pm 8 \text{ ms}$ and $153 \pm 12 \text{ ms}$ (mean \pm s.e.m, $n=6$, where n = number of different clones analysed) respectively. Thus, although we found some correlation between myosin isoform expression and the muscle of origin, all the myotubes expressed slow myosin (MHC1) and this could account for the similarities in their contractile properties.

Supported by BBSRC.

2297-Pos Periodically Arranged Interactions Within The Myosin Thick-Filament Backbone Revealed By Mechanical Unzipping

Brennan J. Decker, Miklos S.Z. Kellermayer

University of Pecs, Pecs, Hungary.

Board B413

Bipolar myosin thick filaments interact with filamentous actin to generate muscle contraction and various forms of cellular motility. Although detailed information is available about the properties of the myosin head domain and its arrangement on the thick-filament surface, the detailed structure of the filament backbone has remained elusive. Based on theoretical analyses it has long been speculated that interaction between periodically arranged charged

regions along the myosin tail forms the basis of filament backbone structure. In the present work we directly tested this long-standing model by mechanically pulling apart synthetic myosin thick filaments using atomic force microscopy and single-filament force spectroscopy. Myosin thick filaments were produced by the precipitation of purified rabbit longissimus dorsi myosin. We found that the unzipping of single myosin thick filaments is accompanied by the appearance of broad force peaks periodically spaced at 4, 14 and 43 nm intervals. This spacing correlates well with the repeat distance of highly-charged regions along the myosin tail. Lowering ionic strength did not change the force-peak periodicity but increased the forces necessary for unzipping. Periodically spaced force peaks were often observed during the mechanical relaxation of thick filaments as well, indicating that the underlying structural transitions are partially reversible. Thus, zipping together of myosin tails is a rapid, spontaneous process, which may play an important role in thick filament formation.

2298-Pos The Effect of Disease Causing Mutations on Sarcomeric Myosin Structure and Function

Thomas Armel

CU Boulder, Boulder, CO, USA.

Board B414

Myosin is the molecular motor of muscle and the structural backbone of the thick filament. Many disease-causing mutations have been discovered in the β -myosin heavy chain gene, which is abundantly expressed in heart and skeletal muscle. While the majority of mutations are located in the motor domain, a number (79) of novel mutations in the coiled coil rod region of β -MyHC have been reported. Although the sequences governing activity of the motor domain have been investigated in detail, relatively less is known about the sequence requirements and mechanisms governing thick filament assembly. This study represents the first attempt to characterize the mechanism(s) of pathogenesis of these mutations. Using an assortment of biophysical assays, we investigated the functional effects of seven mutations that give rise to various clinical phenotypes such as hypertrophic and dilated cardiomyopathies, early onset distal myopathy, and myosin storage myopathy. We show there is a broad spectrum of *in vivo* phenotypes among the seven mutations tested. Circular dichroism experiments suggest an R1500P substitution in the *f* position of the coiled coil affects the α -helical content of the protein, while a L1793P substitution in the *d* position shows no effect. Thermal melts and calorimetry suggest these mutations, along with an R1500W substitution alter the thermal stability. Functional assays using 90 degree light scattering and paracrystal formation to follow self-assembly of the proteins show defects in the ability of L1793P and E1886K proteins to associate into the ordered structures formed by WT myosin. The other three mutations show no detectable phenotype in the assays used. Taken together, these data provide evidence for the underlying cause of several cardiac and skeletal myopathies as well as for the importance of these regions of myosin in proper function of the protein.

2299-Pos Replacing Nonmuscle Myosin II-B with II-A and Nonmuscle Myosin II-A with II-B Using Homologous Recombination

Aibing Wang, Xuefei Ma, Jianjun Bao, Robert S. Adelstein
LMC/GDBC/NHLBI/NIH, Bethesda, MD, USA.

Board B415

We have been interested in learning which of the various functions of nonmuscle myosin II (NM-II) can be replaced by a different isoform *in vivo* during mouse embryonic development. Previous studies showed that ablation of NM II-B was lethal by embryonic day (E)14.5 accompanied by defects in the brain and heart. When we knocked-in cDNA encoding GFP-nonmuscle myosin heavy chain (NMHC) II-A at the II-B gene locus, we were able to rescue defects in cell adhesion in the spinal canal and prevent the hydrocephalus found in II-B ablated mice. In contrast, we were not able to rescue the defect in cardiac myocyte proliferation and most mice die by E14.5 (Bao et al., *J. Biol. Chem.* **282**, 22102, 2007). We interpreted this as reflecting a structural role for NM II in cell adhesion, a function that is independent of the myosin isoform and motor activity. NM II-A null mice die at E6.5 due to defects in the visceral endoderm and cell adhesion in the early embryo. We postulated that the failure of these embryos to undergo gastrulation, a necessary step for organ formation, was partially due to a failure to develop a functional visceral endoderm, since this embryo layer normally lacks NM II-B and II-C and NM II-A was ablated. Expressing GFP-NMHC II-B in place of II-A using homologous recombination allowed the developing embryos to undergo gastrulation and resulted in organ formation, though the mice died by E10. These experiments confirm the importance of NM II for visceral endoderm function in early mouse development and show that its normal function is independent of NM II isoform. Likewise, replacement of NM II-A by II-B rescued cell adhesion defects found in the early II-A ablated embryo.

2300-Pos Biophysics of MyoA: The Molecular Motor Involved in Malarial Parasite Invasion

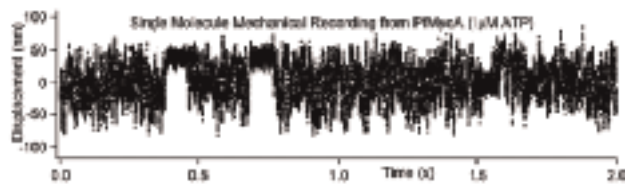
Rachel E. Farrow, Jeremy A. Fielden, Munira Grainger, Judith L. Green, Anthony A. Holder, Justin E. Molloy

MRC NIMR, London, United Kingdom.

Board B416

Myosins form a diverse superfamily of motor proteins capable of translocating actin filaments using the energy of ATP hydrolysis. *Plasmodium falciparum* myosin A (PfMyoA) is a class 14 myosin implicated in the invasion of erythrocytes by malarial merozoites. We have used an *in vitro* motility assay and optical trapping nanometry to investigate the properties of PfMyoA purified from merozoites. Myosin purified from merozoites was adhered to a microscope coverslip using antibodies raised to the myosin tail interacting protein (MTIP). Fluorescence video microscopy was

then used to observe movement of rhodamine-phalloidin labelled actin filaments in the presence of Mg.ATP. We found that the sliding velocity was 3.5 $\mu\text{m/s}$, similar to that of fast skeletal muscle myosin and consistent with the speed at which the merozoite penetrates the erythrocyte. We have used an optical tweezers device to measure the movement produced by a single PfMyoA as it interacts with actin (see figure). The observed, intermittent, binding interactions allow amplitude and kinetics of the working-stroke to be measured. We are expressing PfMyoA in a heterologous system to study transient kinetic properties of its ATPase pathway and effects of small molecule inhibitors.



2301-Pos Restricted Expression of Sarcomeric Protein Isoforms

Peter J. Reiser, Sabahattin Bicer

Ohio State University, Columbus, OH, USA.

Board B417

Virtually all sarcomeric proteins are expressed as families of isoforms. The expression of specific isoforms of a given sarcomeric protein is developmentally regulated and is generally segregated into either fast-type or slow-type muscle fibers. Given the number of isoforms of all of the sarcomeric proteins that could potentially be expressed, there is a general impression that the number of combinations of sarcomeric protein isoforms among mammalian muscle fibers is very large. The goal of this project was to determine the actual number of different types of fast fibers that exist in adult rat limb muscles. Single skinned muscle fibers were isolated and each fiber was analyzed with SDS-PAGE, using two gel formats - one to determine the isoform composition of myosin heavy chain (MHC) and the other to determine isoforms of myosin light chains (MLC), tropomyosin, and troponin (Tn) subunits. The results indicate that some fast fibers express fast and slow isoforms of MLC1, as well as fast MLC2 and MLC3. Multiple fast isoforms of MHC and of TnT were also observed among individual fibers, as expected. However, only a limited number of combinations of specific isoforms of each contractile protein in individual fibers was observed. For example, slow MLC1 was always associated with only MHC-IIA and/or MHC-IID, but never with MHC-IIB. Likewise, three patterns of multiple TnT isoforms were observed among single fast fibers, but each pattern was associated with a specific pattern of MHC isoform expression. The results indicate that there are strict limits on the combinations of sarcomeric protein isoforms among fast fibers, with the end result being a much smaller number of fast fiber types

actually being present than might otherwise exist with a system operating with less stringent control of gene expression.

Supported by the National Science Foundation.

2302-Pos Energy Transduction in Muscle Contraction

Hirofumi Onishi¹, Manuel F. Morales²

¹ERATO Actin-Filament Dynamics Project, JST, Hyogo, Japan,

²University of the Pacific, San Francisco, CA, USA.

Board B418

In muscle contraction, myosin delivers mechanical impulses to an actin filament. The free energy required comes from the ATP hydrolysis by myosin. However, the mechanical process is triggered by actin. A myosin head, bearing ADP-P_i, first attaches to a pair of actins weakly, and then causes closure of the deep ("actin-binding") cleft within the 50-kDa domain. The closure is part of transiting from the weak- to strong-binding state of the actin-myosin complex, which accelerates P_i release from the active site and generates the power stroke of the lever arm. To understand how binding forces generated at the interface cause the cleft closure, we examine the native of both the weak- and strong-binding complexes. Previously, we made mutations at myosin surface loops inferred from crystallography as involved in interactions with the two actins, and tested function defects created by these mutations. Our studies informed about the role of each myosin loop, which had been mutated, and suggested whether it is involved in the weak- or the strong-binding complex. We here present a structure model of the weak-binding complex using knowledge from mutation studies, as well as conventional biochemical and X-ray diffraction studies. From comparing this model with the rigor complex model published earlier, we infer what occurs between the two complexes. Based on these studies, we suggest that state change occurs by attachment of a hydrophobic triplet (Trp-546, Phe-547, and Pro-548) of myosin to an actin conduit with a hydrophobic guiding rail (Ile-341, Ile-345, Leu-349, and Phe-352) and the subsequent linear movement of the triplet along the rail. This attachment creates a great increase in configurational entropy of the complex, which may generate a driving force that causes many changes in the myosin head, viz., the cleft closure, P_i release, and mechanical impulse.

2303-Pos Blebbistatin Inhibits The Chemotaxis Of Vascular Smooth Muscle Cells Through Breaking The Interaction Between Smooth Muscle Myosin II And Actin

Hong Hui Wang¹, Hideyuki Tanaka², Xiaoran Qin^{1,3}, Tiejun Zhao^{1,3}, Lihong Ye^{1,3}, Tuyoshi Okagaki⁴, Takeshi Katayama¹, Akio Nakamura¹, Ryoki Ishikawa¹, Sean E. Thatcher⁵, Gary L. Wright⁵, Kazuhiro Kohama^{1,6}

¹ Department of Molecular and Cellular Pharmacology, Gunma University Graduate School of Medicine, Maebashi, Japan,

² Department of Research Science, Gunma University School of Health Sciences, Maebashi, Japan,

³ Department of Biochemistry, College of Life Sciences, Nankai University, Tianjin, China,

⁴ Department of Bioresources, Mie University, Tsu, Japan,

⁵ Department of Physiology, The Joan Edwards School of Medicine, Marshall University, Huntington, WV, USA,

⁶ Department of Biological Sciences, Laboratory of Molecular Physiology, Marshall University, Huntington, WV, USA.

Board B419

Blebbistatin is a myosin II-specific inhibitor. However, the mechanism and tissue specificity of the drug are not well understood. Blebbistatin blocked the chemotaxis of vascular smooth muscle cells (VSMCs) toward both sphingosylphosphorylcholine ($IC_{50} = 26.1 \pm 0.2 \mu M$ for GbaSM-4 cells and $27.5 \pm 0.5 \mu M$ for A7r5 cells) and platelet-derived growth factor BB ($IC_{50} = 32.3 \pm 0.9 \mu M$ for GbaSM-4 cells and $31.6 \pm 1.3 \mu M$ for A7r5 cells) at similar concentrations. Immunofluorescence and fluorescent resonance energy transfer analysis indicated that blebbistatin caused a disruption in the actin-myosin interaction in VSMCs. Subsequent experiments indicated that blebbistatin inhibited the Mg^{2+} -ATPase activity of both the unphosphorylated ($IC_{50} = 12.6 \pm 1.6 \mu M$ for gizzard and $4.3 \pm 0.5 \mu M$ for bovine stomach) and phosphorylated ($IC_{50} = 15.0 \pm 0.6 \mu M$ for gizzard) forms of purified smooth muscle myosin II, suggesting a direct effect on myosin II motor activity. It was further observed that the Mg^{2+} -ATPase activities of gizzard myosin II fragments, heavy meromyosin ($IC_{50} = 14.4 \pm 1.6 \mu M$) and subfragment 1 ($IC_{50} = 5.5 \pm 0.4 \mu M$) were also inhibited by blebbistatin. Assay by *in vitro* motility indicated that the inhibitory effect of blebbistatin was reversible. Electron microscopic evaluation showed that blebbistatin induced a distinct conformational change (swelling) of the myosin II head. The results suggest that the site of blebbistatin action is within the S1 portion of smooth muscle myosin II.

Actin & Actin-binding Proteins

2304-Pos Coronin-1A Stabilizes F-Actin by Bridging Adjacent Actin Protomers and Stapling Opposite Strands of the Actin Filament

Vitold E. Galkin¹, Albina Orlova¹, William M. Briehner², Timothy J. Mitchison², Edward H. Egelman¹

¹ University of Virginia, Charlottesville, VA, USA,

² Harvard Medical School, Boston, MA, USA.

Board B419.01

Coronins are F-actin binding proteins that are involved, in concert with Arp2/3, Aip1 and ADF/cofilin, in rearrangements of the actin cytoskeleton. An understanding of coronin function has been ham-

pered by the absence of any structural data on its interaction with actin. Using electron microscopy and three-dimensional reconstruction, we show that coronin-1A binds to three protomers in F-actin simultaneously: it bridges subdomain 1 and subdomain 2 of two adjacent actin subunits along the same long-pitch strand, and it staples subdomain 1 and subdomain 4 of two actin protomers on different strands. Such a mode of binding explains how coronin can stabilize actin filaments *in vitro*. In addition, we show which residues of F-actin may participate in the interaction with coronin-1A. Human nebulin and Xin, as well as *Salmonella* invasion protein A (SipA) use a similar mechanism to stabilize actin filaments. We suggest that the stapling of subdomain 1 and subdomain 4 of two actin protomers on different strands is a common mechanism for F-actin stabilization utilized by many actin binding proteins that have no homology.

2305-Pos Widely-distributed Residues In Thymosin $\beta 4$ Are Critical For Actin Binding

Joshua K. Au¹, Daniel Safer², Enrique M. De La Cruz¹

¹ Yale University, New Haven, CT, USA,

² University of Pennsylvania, Philadelphia, PA, USA

Board B420

We have investigated the contributions of hydrophobic residues, the conserved and variable proline residues, and the conserved lysine residues to the kinetics and thermodynamics of thymosin $\beta 4$ (T $\beta 4$) binding to MgATP-actin monomers. Pro4, Lys18, Lys19, Pro27, Leu28, Pro29, and Ile34 were substituted by alanine residues. Mutagenesis of Pro 4 or Pro27 has little effect (≤ 3 -fold reduction) on the actin binding affinity of T $\beta 4$. Substitution of Lys18 and Lys19, Leu28, Pro29 or Ile34 weaken the affinity of the actin-T $\beta 4$ complex ≥ 10 -fold, but the kinetic basis of the lower stability varies among the mutants. Substitution of the conserved Lysine residues weakens the affinity by slowing association. Substitution of hydrophobic residues Leu28 or Ile34 weaken the affinity by accelerating dissociation. These results favor a reaction mechanism in which T $\beta 4$ initially binds actin monomers through an electrostatic interaction, followed by isomerization to a strong binding state that is coupled to the formation of widely-distributed hydrophobic contacts. The isomerization equilibrium is slowed by mutagenesis of Pro27. Mutagenesis of Pro4 or Pro27 accelerates binding and dissociation but minimally affect the binding affinity (≤ 3 -fold reduction), suggesting that *cis-trans* isomerization at proline residues contribute to the slow association rate constant of T $\beta 4$.

2306-Pos The Actin Severing Protein, Cofilin, Modulates the Mechanical Properties of Actin Filaments

Brannon McCullough, Enrique M. De La Cruz

Yale University, New Haven, CT, USA.